

A Simple Unified Framework for Anomaly Detection in Deep Reinforcement Learning

Hongming Zhang^{1*}, Ke Sun^{2*}, Bo Xu³, Linglong Kong², Martin Müller¹

¹ Department of Computing Science, University of Alberta

² Department of Mathematical and Statistical Sciences, University of Alberta

³ Institute of Automation, Chinese Academy of Sciences

{hongmin2, ksun6, lkong, mmueller}@ualberta.ca, boxu@ia.ac.cn

Abstract

Abnormal states in deep reinforcement learning (RL) are states that are beyond the scope of an RL policy. Such states may make the RL system unsafe and impede its deployment in real scenarios. In this paper, we propose a simple yet effective anomaly detection framework for deep RL algorithms that simultaneously considers random, adversarial and out-of-distribution (OOD) state outliers. In particular, we attain the class-conditional distributions for each action class under the Gaussian assumption, and rely on these distributions to discriminate between inliers and outliers based on Mahalanobis Distance (MD) and Robust Mahalanobis Distance. We conduct extensive experiments on Atari games that verify the effectiveness of our detection strategies. To the best of our knowledge, we present the first in-detail study of statistical and adversarial anomaly detection in deep RL algorithms. This simple unified anomaly detection paves the way towards deploying safe RL systems in real-world applications.

1 Introduction

Deep Reinforcement Learning (RL) algorithms vary considerably in their performance and tend to be highly sensitive to a wide range of factors, including the environment, state observations and hyper-parameters (Henderson et al. 2018; Jordan et al. 2020). Such lack of robustness of RL algorithms hinders their deployment in practical scenarios, especially in safety-critical applications, such as autonomous driving. Recently, the reliability of RL algorithms has gained substantial attention (Chan et al. 2019; Duan et al. 2016; Colas, Sigaud, and Oudeyer 2018), and detection-based strategies are crucial for constructing trustworthy RL systems. For instance, reward deterioration detection (Greenberg and Manor 2021) can be widely applied to detect changes or drifts in any episodic signal. Additionally, observed states might contain natural measurement errors (random noises), adversarial perturbations, and even out-of-distribution observations. Such abnormal state observations deviate from true states, and they can mislead the agent into choosing suboptimal actions beyond the scope of its policy. We claim that detecting abnormal states should play a key role in developing trustworthy RL systems for real-world applications.

In the deep learning literature, a simple yet effective detection approach (Lee et al. 2018) in image classification is the closest to our study. They designed a confidence score based on Mahalanobis Distance (MD) (De Maesschalck, Jouan-Rimbaud, and Massart 2000) for detecting both out-of-distribution and adversarial samples. Their detection strategy is based on the assumption that class-conditional distributions of pre-trained features have a “tied” covariance. This assumption is considered implausible by (Kamoi and Kobayashi 2020) who demonstrated that MD is capable of making use of the information in intermediate features that is not utilized as much for classification. Besides, MD was also employed to detect near OOD inputs in neural networks (Ren et al. 2021).

Robust statistical methods (Huber 2004) have been developed for a wide range of common problems, such as estimating location and scale. One motivation of robust estimation is to produce statistical methods that are not unduly affected by outliers. In particular, robust estimators for location and covariance have been introduced in (Maronna and Yohai 2014), and the most frequently used in practice is the minimum covariance determinant (MCD) estimator (Rousseeuw 1984). These results motivate us to examine the effectiveness of both MD and Robust MD in anomaly detection for RL. Figure 1 shows contours computed by both methods for state feature vectors on Breakout game. It illustrates that estimation based on Robust MD is less vulnerable to outlying states (red points), and fits inliers (black points) much better than MD, showing its potential advantage in the RL outlier detection.

In this paper, we design a simple yet effective and unified anomaly detection framework in the deep RL scenario. We propose MD and robust MD-based detection strategies that simultaneously discriminate random, adversarial and out-of-distribution state outliers in both the *evaluation* and the *training* phase of an RL algorithm. We avoid using the implausible “tied” covariance assumption (Lee et al. 2018) in our detection strategy, and instead approximate the penultimate feature distribution of state observations by a single Gaussian distribution for each action class. *Moving window estimation* and *double self-supervised detectors* are incorporated into our online detection approach in the training. In experiments, we demonstrate that the robust MD-based detection strategy outperforms its non-robust counterpart when

*These authors contributed equally.
Preprint. Under review.

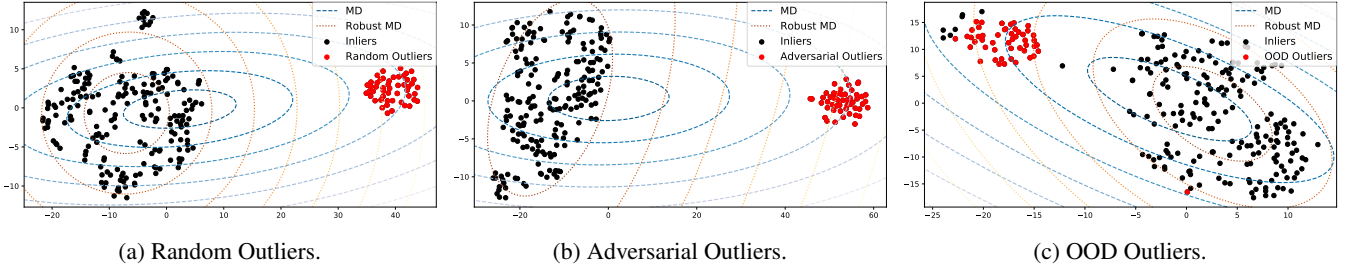


Figure 1: Contours under the estimation based on MD and Robust MD across different outliers on Breakout. Black and red points denote inliers and outliers. The dimension of state feature vectors after a pre-trained PPO policy is reduced by t-SNE.

the agent observes a fraction of contaminated state observations in the evaluation phase. Additionally, we also verify that our online detection strategy, which deletes the detected state outliers, can mitigate the performance decline of RL algorithms and thus improve their final performance under the outlier exposure.

2 Preliminaries

In this section, we will recap the classical Markov Decision Process (MDP) setting in RL, and review relevant technical details of the Proximal Policy Optimization (PPO) algorithm, and introduce the three kinds of outliers in our anomaly detection framework.

Markov Decision Process (MDP)

In the tabular setting, the interaction of an agent with its environment can be modeled as a Markov Decision Process (MDP), a 5-tuple $(\mathcal{S}, \mathcal{A}, R, P, \gamma)$. \mathcal{S} and \mathcal{A} are the state and action spaces, $P : \mathcal{S} \times \mathcal{A} \times \mathcal{S} \rightarrow [0, 1]$ is the environment transition dynamics, $R : \mathcal{S} \times \mathcal{A} \times \mathcal{S} \rightarrow \mathbb{R}$ is the reward function and $\gamma \in (0, 1)$ is the discount factor.

Proximal Policy Optimization (PPO)

The actor-critic based policy gradient algorithm Proximal Policy Optimization (PPO) (Schulman et al. 2017) has achieved the state-of-the-art or competitive performance on both Atari games and Mujoco robotic tasks. Typical policy gradient algorithms optimize the average reward function $\rho(\theta, s_0) = \mathbb{E}_{\pi_\theta} [\sum_{t=0}^{\infty} \gamma^t r(s_t) | s_0]$ by leveraging the policy gradient theorem. Here π_θ is the θ -parameterized policy function. Trust Region Policy Optimization (TRPO) (Schulman et al. 2015a) and PPO (Schulman et al. 2017) utilize constraints and advantage estimation to perform the update by reformulating the original optimization problem with the surrogate loss $L(\theta)$ as

$$L(\theta) = \mathbb{E}_t \left[\frac{\pi_\theta(s_t, a_t)}{\pi_{\theta_{\text{old}}}(s_t, a_t)} A_{\pi_{\theta_{\text{old}}}}(s_t, a_t) \right] \quad (1)$$

$$= \mathbb{E}_t [r_t(\theta) A_t(s_t, a_t)],$$

where $A_{\pi_{\theta_{\text{old}}}}$ is the generalized advantage function (GAE) (Schulman et al. 2015b). Further, PPO reformulates the objective function as a clipping one to penalize changes

to the policy that make $r_t(\theta)$ vastly different from 1:

$$\mathbb{E}_t [\min(r_t(\theta) A_t(s_t, a_t), \text{clip}(r_t(\theta), 1 - \epsilon, 1 + \epsilon) A_t(s_t, a_t))]. \quad (2)$$

Transitions are sampled by multiple actors in parallel (Henderson et al. 2018). Although the clipping parameter ϵ has to be pre-determined, PPO has still accomplished promising performance. In this paper, we use PPO as the main algorithm to investigate the efficacy of our anomaly detection framework. However, it can also be easily applied to other typical RL algorithms.

Three Types of Outliers

Random Outliers Random outliers represent state observations with random noises. In particular, we simulate such outliers by applying Gaussian noises with mean 0 and different standard deviations to state observations. This can also simulate measurement errors.

Adversarial Outliers For adversarial outliers, we construct white-box adversarial perturbations (Goodfellow, Shlens, and Szegedy 2014; Szegedy et al. 2013; Cao et al. 2020) on state observations for the current policy, following the strategy proposed in (Huang et al. 2017; Pattanaik et al. 2017). Particularly, we denote a_w^t as the “worst” action, with the lowest probability from the current policy $\pi_t(a|s)$. Thus, the optimal adversarial perturbation η_t , constrained in an ϵ -ball, can be derived by minimizing the objective function J :

$$\min_{\eta} J(s_t + \eta, \pi_t) = - \sum_{i=1}^n p_i^t \log \pi_t(a_i | s_t + \eta), \text{ s.t. } \|\eta\| \leq \epsilon, \quad (3)$$

where $p_i^t = 1$ if i corresponds to the index of the least-chosen action, i.e. the w -th index in the vector a . Otherwise $p_i^t = 0$. We leverage the Fast Gradient Sign Method (FGSM) (Goodfellow, Shlens, and Szegedy 2014) to solve this minimization problem, and obtain adversarial outliers $s_t + \eta_t^*$ that can force the policy to choose the least-chosen action a_w^t .

Out-of-Distribution (OOD) outliers Due to the discrepancy of data distribution among various environments, we randomly draw states from other environments as the OOD outliers for the current environment. Therefore, we can explore the efficacy of our detection strategy regarding out-of-distribution (OOD) outliers.

3 Anomaly Detection in the Evaluation Phase

We design (robust) MD-based detection strategies when the agent exposes *contaminated* states, which contain a fraction of state outliers, in the evaluation phase of RL algorithms.

The Gaussian Assumption

In the evaluation phase, the pre-trained parameterized policy π_θ can be viewed as a discriminative softmax classifier $\pi(a_t = c | s_t) = \frac{\exp(\mathbf{w}_c^\top f(s_t) + b_c)}{\sum_{c'} \exp(\mathbf{w}_{c'}^\top f(s_t) + b_{c'})}$, where \mathbf{w}_c and b_c are the weight and bias of the policy classifier for action class c , and $f(\cdot)$ is the output of the penultimate layer of the policy network π_θ , serving as the state feature vector. Here we denote $C = |A|$ as the size of the action space and μ_c as the mean vector of $f(s)$ falling into the action class c . Following the conclusion from (Lee et al. 2018), if we assume that the class-conditional distribution follows the multivariate Gaussian distribution with a tied covariance Σ in a generative classifier, i.e., $\pi(f(s) | a = c) = \mathcal{N}(f(s) | \mu_c, \Sigma)$, the posterior distribution of $f(s)$ is equivalent to the form of a discriminative softmax classifier. This implies that $f(s)$ might be fitted in Gaussian distribution during training the policy π_θ . However, the tied covariance assumption has been challenged by (Kamoi and Kobayashi 2020) through their visualization experiments. Hence, in our work we approximate state feature vectors with a class-conditional Gaussian distribution for each action class, i.e., μ_c and Σ_c , rather than leverage a “tied” covariance Σ . The effectiveness of our *Gaussian parametric method* in outlier detection is verified in our following experiments.

Mahalanobis Distance

The Gaussian assumption allows the deployment of Mahalanobis distance-based detection that leverages the mean vectors μ_c and the covariance matrix Σ_c to capture the data structure of $f(s)$ in each action class c . Concretely, in the evaluation phase of a RL algorithm, we firstly collect $\{(s_i, a_i)\}$ state action pairs for each action class to estimate the empirical class mean and covariance:

$$\begin{aligned} \hat{\mu}_c &= \frac{1}{N_c} \sum_{i:a_i=c} f(s_i), \\ \hat{\Sigma}_c &= \frac{1}{N_c} \sum_{i:a_i=c} (f(s_i) - \hat{\mu}_c)(f(s_i) - \hat{\mu}_c)^\top, \end{aligned} \quad (4)$$

where N_c is the number of $\{(s_i, a_i)\}$ pairs collected in advance for the action class c . Compared with Euclidean distance, Mahalanobis distance utilizes additional information of data covariance to normalize the distance into a more comparable scale. This explains the superiority of Mahalanobis distance over Euclidean distance in many tasks (Lee et al. 2018; Ren et al. 2021; Kamoi and Kobayashi 2020).

After the estimation in Eq. 4, we obtain the class-conditional Gaussian distribution to describe the main data structure in the state representation space for each action class. For each state s that the agent observes, we compute *Detection Mahalanobis Distance* $M(s)$ by using the Maha-

lanobis distance between the state s and the closest class-conditional Gaussian distribution:

$$M(s) = \max_c - (f(s) - \hat{\mu}_c)^\top \hat{\Sigma}_c^{-1} (f(s) - \hat{\mu}_c). \quad (5)$$

Previous work (Lee et al. 2018) leveraged a Mahalanobis confidence score to further construct a binary (logistic) classifier in the image classification task. This approach heavily relies on the validation dataset. In stark contrast, we utilize $M(s)$ as the detection metric under the statistical hypothesis test framework. As suggested in the following Proposition 1, the detection metric, i.e., Detection Mahalanobis Distance $M(s)$, is Chi-squared distributed under the Gaussian assumption.

Proposition 1. (*Relationship between Detection Mahalanobis distance and Chi-Squared distribution*) Let $f(s)$ be the p -dimensional state random vector for action class c . Under the Gaussian assumption, i.e., $P(f(s) | a = c) = \mathcal{N}(f(s) | \mu_c, \Sigma_c)$, Detection Mahalanobis Distance $M(s)$ in Eq. 5 is Chi-Square distributed, i.e., $M(s) \sim \chi_p^2$.

Please refer to Appendix A for the proof. Based on Proposition 1, we can select a critical value in the specified Chi-Squared distribution to separate the normal states from outliers. In particular, given a confidence level $1 - \alpha$, if $M(s) > \chi_p^2(1 - \alpha)$ for a new state observation s , then the state s is detected as an outlier. In our experiments, we provide detection results over a series of p values on the Chi-Squared distribution.

Robust Mahalanobis Distance

The estimation of μ_c and Σ_c in Eq. 4 is based on Maximum Likelihood Estimate (MLE). It is well-known that MLE is sensitive to the presence of outliers in the data set (Rousseeuw and Van Zomeren 1990; Cabana, Lillo, and Laniado 2021) and therefore, the downstream Mahalanobis distances also are. In our outlier scenarios, the agent sequentially gets exposed to outliers in the evaluation phase. The contaminated state observations that agent observes motivate us to leverage a robust estimator to make the resulting estimation resistant to extreme state observations. Therefore, we select Robust Mahalanobis Distance (Rousseeuw 1984; Huber 2004) as our robust metric while designing our detection strategies in order to more accurately reflect the true structure of the state observations in the state representation space.

The Minimum Covariance Determinant (MCD) estimator (Rousseeuw 1984; Grübel 1988) is a robust estimator, which can be used to estimate the robust mean vector and covariance matrix of a highly contaminated dataset. MCD determines the subset J of observations of size h that minimizes the determinant of the sample covariance matrix, computed from only these h points. The choice of h determines the trade-off between the robustness and efficiency of the estimator. Therefore, the robust MCD mean vector $\hat{\mu}_c^{\text{MCD}}$ and covariance matrix $\hat{\Sigma}_c^{\text{MCD}}$ in the action class c are computed as

$$J = \left\{ \text{set of } h \text{ points} : \left| \widehat{\Sigma}_J \right| \leq \left| \widehat{\Sigma}_K \right| \text{ for all subsets } K \right\},$$

$$\widehat{\mu}_c^{\text{MCD}} = \frac{1}{h} \sum_{i:i \in J, a_i = c} f(s_i),$$

$$\widehat{\Sigma}_c^{\text{MCD}} = \frac{1}{h} \sum_{i:i \in J, a_i = c} (f(s_i) - \widehat{\mu}_c^{\text{MCD}}) (f(s_i) - \widehat{\mu}_c^{\text{MCD}})^\top.$$

Based on the robust estimation of mean and covariance matrix, we similarly define *Detection Robust Mahalanobis Distance* $M_{\text{MCD}}(s)$ as another robust outlier detection metric:

$$M_{\text{MCD}}(s) = \max_c - (f(s) - \widehat{\mu}_c^{\text{MCD}})^\top \widehat{\Sigma}_c^{\text{MCD}-1} (f(s) - \widehat{\mu}_c^{\text{MCD}}). \quad (7)$$

Since the robust Mahalanobis distance can still approximate the true Chi-squared distribution, we still use the threshold value $\chi_p^2(1 - \alpha)$ for detecting outliers as in the Mahalanobis distance case.

MD-based Detection Algorithm in Evaluation

A key issue we need to consider while deploying the detection method is its computational efficiency. We apply Principal Components Analysis (PCA) on the p -dimensional state feature vectors in the penultimate layer of π_θ , and conduct MD-based detection in the resulting lower-dimensional representation space. Figure 2 shows a detailed explanation of the outlier detection pipeline in the evaluation phase.

- In the first estimation phase, when the agent exposes the contaminated state observations, we perform the (robust) estimation on the mean vector and covariance matrix within each action class under the Gaussian assumption.
- In the second evaluation phase, given a new state observation s , we evaluate the detection metrics $M(s)$ and $M_{\text{MCD}}(s)$ via Eq. 5 and 7. Finally, comparison with a threshold value $\chi_p^2(1 - \alpha)$ with a pre-specified confidence level $1 - \alpha$ determines whether the state s is an outlier or not.

Remark. We consider a *balanced* amount of normal (inliers) and abnormal (outliers) state observations to evaluate

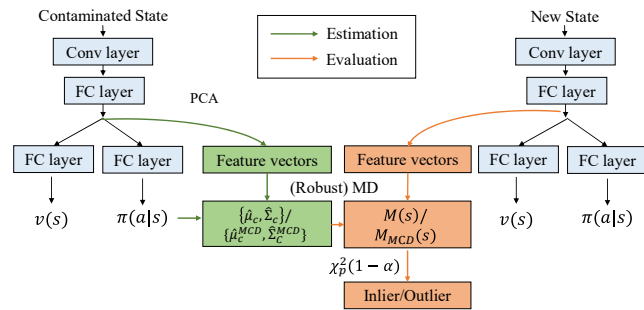


Figure 2: MD-based anomaly detection pipeline in the evaluation phase of the PPO algorithm.

Algorithm 1: MD-based Detection Algorithm in Evaluation

Input: The pre-trained policy π_θ , the reduced dimension of state feature vectors from p to k , and a confidence level $1 - \alpha$.
Output: Detection labels $\{y_s\}$ for each s in the evaluation trajectory.

```

1: /* (Robust) Mean and Covariance Estimation */
2: Collect state action pairs  $\{(s_i, a_i)\}$  where  $a_i \sim \pi_\theta(\cdot | s_i)$ .

3: for each action class  $c$  do
4:   if we choose MD detection then
5:     Estimate  $\widehat{\mu}_c$  and  $\widehat{\Sigma}_c$  via Eq. 4.
6:   else
7:     Estimate  $\widehat{\mu}_c^{\text{MCD}}$  and  $\widehat{\Sigma}_c^{\text{MCD}}$  via Eq. 6.
8:   end if
9: end for

10: /* Detection */
11: for each states  $s$  in the following evaluation phase do
12:   Evaluate  $M(s)$  via Eq. 5 or  $M_{\text{MCD}}(s)$  via Eq. 7.
13:   Detection labels  $y_s = 1$  if  $M(s) > \chi_k^2(1 - \alpha)$ 
       ( $M_{\text{MCD}}(s) > \chi_k^2(1 - \alpha)$ ) else  $y_s = -1$ .
14: end for

```

the real detection performance for our detection strategies, although in real scenarios the agent often faces a contaminated data stream with a (nearly) constant fraction of outliers (Feng et al. 2013). A detailed practical algorithm is given in Algorithm 1.

4 Anomaly Detection in the Training Phase

Training robustness is increasingly important in safe RL, as the agent is more likely to encounter state outliers during training. In this section we extend the MD-based detection approach to the training phase. We use the two techniques of *Moving Window Estimation* and *Double Self-supervised Detectors*. Both are pivotal for the empirical success of our anomaly detection framework.

Moving Window Estimation

One crucial hurdle in the online setting is that improving the policy π_θ leads to changing of the data distribution when the agent interacts with the environment. To leverage the information from the updated data distribution, we perform a moving window estimation of PCA and MD. In particular, PCA is updated only infrequently (every few hundred iterations) and based on the constantly updated lower-dimensional state feature vectors, μ_c and Σ_c (μ_c^{MCD} and Σ_c^{MCD}) are further estimated. This type of update resembles the target network in Deep Q Network (Mnih et al. 2015), which yields the stability.

Double Self-Supervised Detectors

Once we have successfully detected outliers during training, there are multiple options we can choose to handle them, such as direct removal or outlier filling. We focus on directly getting rid of detected outliers, and evaluate the resulting training curve of cumulative rewards. A good detector should recognize outliers accurately, and largely elimi-

Algorithm 2: MD-based Detection Algorithm in Training on PPO, Actor-Critic Style

Randomly initialize policy network π_θ .

Initialize confidence level $1-\alpha$ and moving window size m .

Initialize inlier and outlier buffers $\mathcal{B}_I, \mathcal{B}_O$ with size $C \cdot m \cdot N_c$.

```

1: for iteration=1, 2, ...,  $K$  do
2:   for actor=1, 2, ...,  $N$  do
3:     Run policy  $\pi_\theta$  in environment for  $T$  timesteps.
4:     Compute advantage estimates  $\hat{A}_1, \dots, \hat{A}_T$ .
5:     if iteration  $\leq K/2$  then
6:       Add inlier trajectory to  $\mathcal{B}_I$  and optimize policy
        $\pi_\theta$  using inlier trajectory automatically.
7:     else
8:       Reduce feature dimension from  $p$  to  $k$  by PCA.
9:       Evaluate the trajectory via MD metrics.
10:      if  $M(s)$  or  $M_{MCD}(s) \leq \chi_p^2(1-\alpha)$  then
11:        Add it to  $\mathcal{B}_I$ .
12:      else
13:        Add it to  $\mathcal{B}_O$ .
14:      end if
15:      Optimize policy  $\pi_\theta$  using inlier trajectory.
16:      Update the  $\hat{\mu}_c$  and  $\hat{\Sigma}_c$  ( $\hat{\mu}_c^{MCD}$  and  $\hat{\Sigma}_c^{MCD}$ ) estimation
      of the two detectors on  $\mathcal{B}_I$  and  $\mathcal{B}_O$  respectively every  $C \cdot N_c$  samples.
17:    end if
18:  end for
19: end for

```

nate the impact of these abnormal samples on the training. At the beginning of a training process, our detection efficacy is limited by the performance of the policy. The resulting unreliable detector may fail to exclude the outliers in the training data and even erroneously exclude true informative clean data. This can destabilize the algorithm and even worsen its final performance. To address this issue, we derive another

detector based on the detected outlier buffer \mathcal{B}_O by the original detector, which thus works in a self-supervised manner. The new self-supervised detector can adjust the detection errors from the first detector. We demonstrate the effectiveness of our double self-supervised detectors through our extensive experiments and provide the ablation study in Appendix F.

MD-based Detection Algorithm in Training

Algorithm 2 shows our MD-based Detection algorithm in training, combined with moving window estimation and double self-supervised techniques. Inliers and outliers in buffers \mathcal{B}_I and \mathcal{B}_O are used to update our double detectors. mN_c state action pairs are used to estimate $\hat{\mu}_c$ and $\hat{\Sigma}_c$ ($\hat{\mu}_c^{MCD}$ and $\hat{\Sigma}_c^{MCD}$) for each class, where m is the moving window size. Within each moving window update, for each action class c , N_c states will be newly collected while maintaining the previous $(m-1)N_c$ states. In a real scenario, such as a recommendation system, we would normally deploy a pre-trained policy at first in the online system to recommend items for each user in real time. Next, the feedback, such as the click-through rate (CTR), will be observed to update the policy in an online manner. Similarly, in our online detection algorithm, a randomly initialized policy π_θ is firstly trained excluding outliers in the first half of the training phase. Then our MD-based detection algorithm is further used to detect outliers in the following online training process. Finally, we evaluate the training performance of algorithms under our detection strategies.

5 Experiments

We conduct extensive experiments on the three Atari games, including Breakout, Asterix and SpaceInvaders, to verify the outlier detection effectiveness of both our MD and Robust MD detection strategies in both the evaluation and training phases.

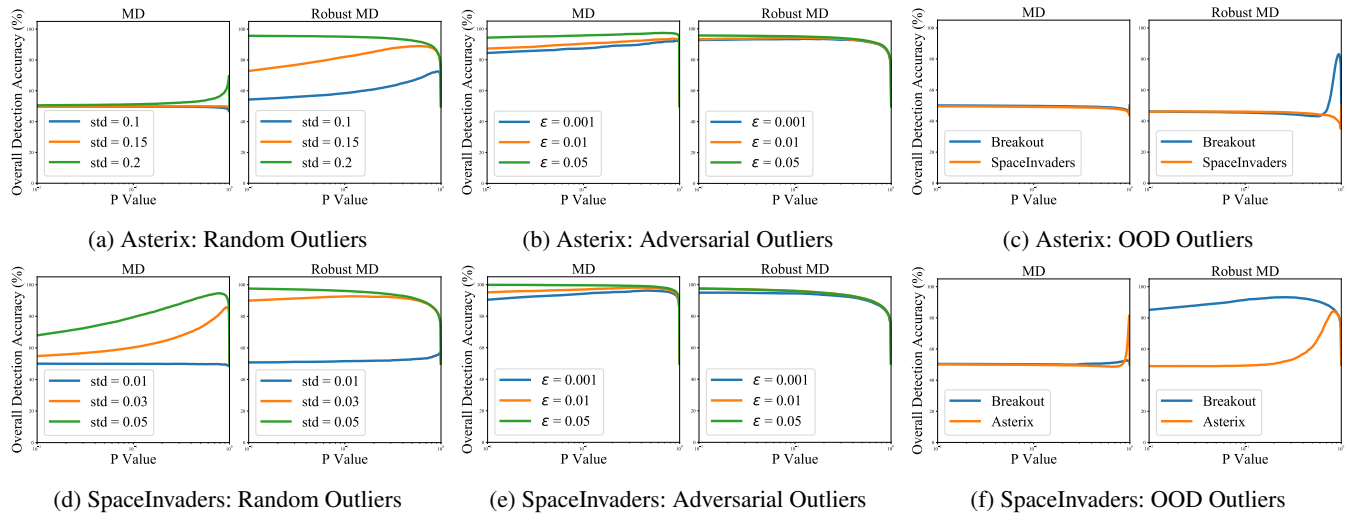


Figure 3: Detection performance in the evaluation phase over various abnormal states across a series of p-values (10^{-2} to 1.0) in $\chi_k^2(1-\alpha)$ on Asterix and SpaceInvaders games with a 0.01 fraction of contamination.

Anomaly Detection in the Evaluation Phase

Main Results. We illustrate the outlier detection effectiveness of our MD and robust MD strategies across different proportions of outlier exposure. In the first estimation phase we collect $\{(s_t, a_t)\}$ pairs in the replay buffer when the agent interacts with the environment, which contains a fraction λ of one specific type of abnormal states, such as adversarial outliers. Next, based on this contaminated dataset, we leverage PCA to reduce the state feature vectors into a 50-dimensional space, then apply MD and Robust MD to estimate mean vectors and covariances. Finally, we evaluate the performance of our detection methods on a balanced new state set with 50% outliers. Given a new state s , we compute the detection metric $M(s)$ and $M_{\text{MCD}}(s)$, respectively, and utilize $\chi^2_{50}(1 - \alpha)$ for the detection.

Figure 3 displays that the detection performance of Robust MD is superior to the classical MD across all types of outliers with a 0.01 fraction of contamination on Asterix and SpaceInvaders games. Due to the space limit, we provide the similar results on Breakout in Figure 10 of Appendix B. The superior overall detection accuracy of robust MD-based detection over classical MD holds across a wide range of p values in $\chi^2_{50}(1 - \alpha)$. We do not naively use the standard rule of $\alpha = 0.05$ as our detection metric since the best detection performance over all p values depends on the task and type of outliers. We leave the best option of the detection metric α as future work.

We also provide similar results on the three games without contamination in Figure 11 and with 0.05 and 0.1 fractions of contamination in Figure 12 and 13 in Appendix B. Robust MD outperforms MD in most cases especially for adversarial outliers, although both strategies tend to degrade as the proportion of contamination increases.

The Power of Robust MD to Detect Outliers. The power of Robust MD to detect outliers lies in the fact that the distribution of outlier states can be more separated from the distribution of inlier states under Robust MD. To demonstrate this claim, we take the cubic root of the Mahalanobis distances, which yields approximately normal distributions (Wilson and Hilferty 1931). In this experiment, 250 clean states are drawn from the replay buffer, combined with 50 abnormal states from each of the three types of outliers. We use t-SNE to reduce the dimension of state feature vectors of both inlier and outlier states into two. Next, we compute Maha-

lanobis distances of these two kinds of states to their centrality within each action class under the estimation based on MD or Robust MD, respectively. Figure 4 clearly illustrates that Robust MD separates inliers and outliers much better than MD on Breakout game within a random action class. This implies that robust MD facilitates their identification in the detection. Similar results for Asterix and SpaceInvaders are provided in Appendix C.

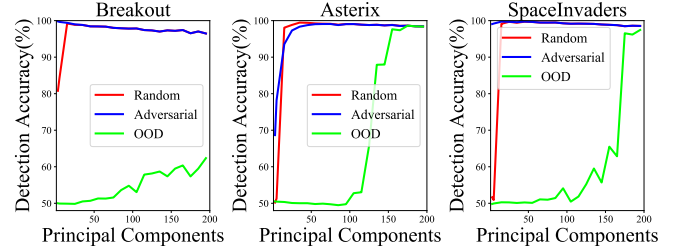


Figure 5: Detection performance under Robust MD estimation as the number of principal components increases across Breakout, Asterix and SpaceInvaders.

Sensitivity Analysis on Principal Components. The impact of the number of principal components on the detection performance is shown in Figure 5. The detection accuracy over all considered outliers tends to improve with the number of principal components, except for a slight decline for random and adversarial outliers (red and blue lines) on Breakout game. The increase implies that the subspace spanned by principal components with small explained variance also contains useful information for detecting anomalous states from in-distribution states, which coincides with the conclusion in (Kamoi and Kobayashi 2020). We provide a similar result for MD estimation in Appendix D.

Anomaly Detection in the Training Phase

Main Results. Owing to the parallel computation of PPO and the estimation of GAE, we run eight environments in parallel as in the original paper, and add state outliers on all state observations in four environments. For OOD outliers, we draw the OOD state from a different environment after randomly choosing actions from the action space in the OOD environment. We consider discriminating states trajectory by trajectory and regard a trajectory as outliers if half of

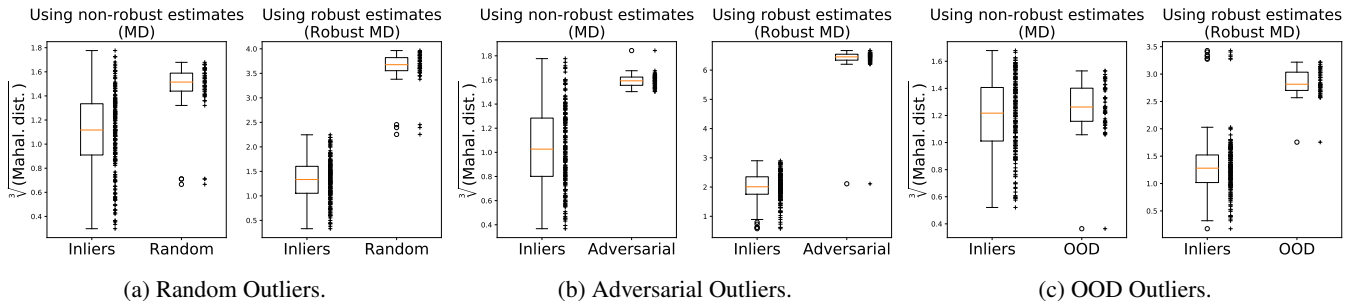


Figure 4: Boxplot of distributions between inliers and three types of outliers in a random action class on Breakout game.

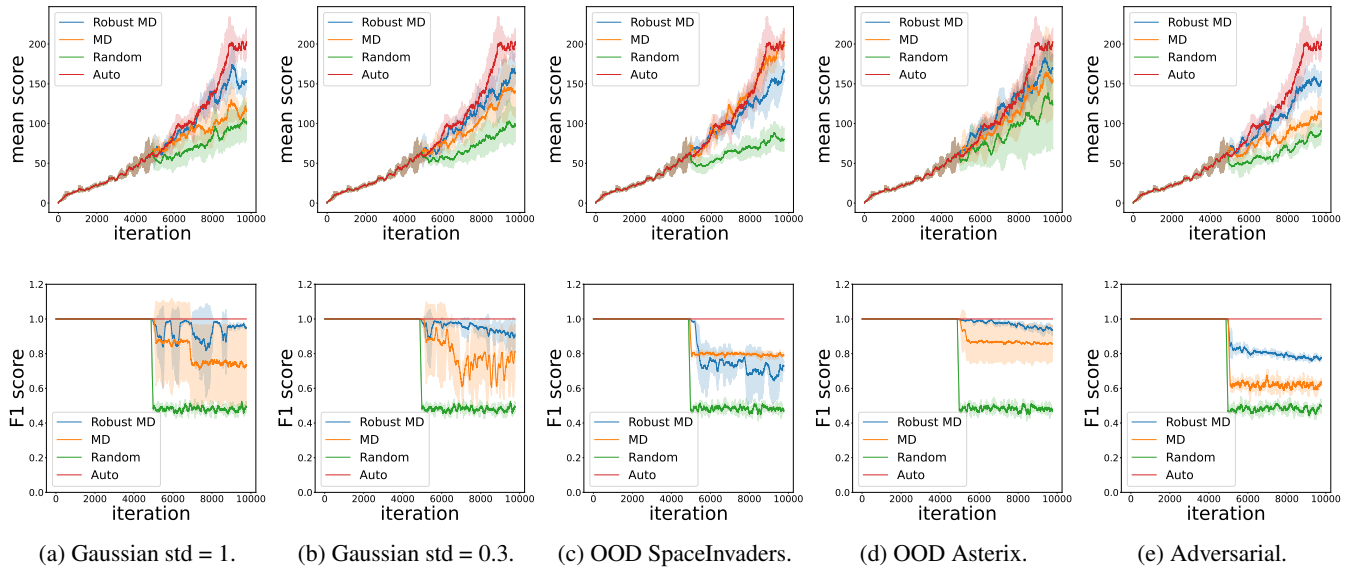


Figure 6: Detection performance of MD and robust MD strategies across various state outliers in the training phase on Breakout. “Mean score” in the first row indicates the accumulated rewards of PPO, while “F1 Score” in the second row evaluates the detection performance during PPO training.

its states are classified as anomaly. Hyper-parameters details are provided in Table 1 in Appendix E.

Figure 6 shows the variation of cumulative rewards (first row) of PPO and F1 scores (second row) of detection under different detection methods on Breakout. For an ideal baseline, the method “Auto” deletes true added state outliers, showing the best training performance of algorithms without the interruption from outliers. As the other extreme, “Random” uses a totally random detector. The performance curves of MD and Robust MD are between two curves of “Auto” and “Random”, indicating that both of our strategies effectively detect outliers and stabilize the training of algorithms. We provide similar results for Asterix and SpaceInvaders in Appendix E.

Ablation Study on Different Proportions of Contamination. We study different contamination ratios that the agent encounters in the training process. We train PPO on

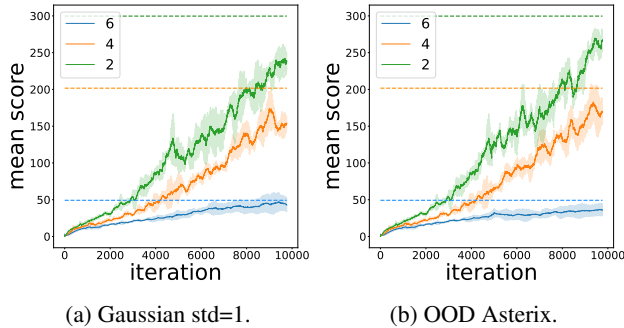


Figure 7: Training performance under robust MD detection under different proportions of outlier exposure on Breakout.

two, four or six noisy environments among all eight parallel environments. Figure 7 suggests that the training performance under our robust MD detection evenly degrades as the contamination ratio increases. The dashed lines indicate the performance of the oracle “Auto” detector. The training performance of our detection gradually approaches the ideal performance. And we also conduct an ablation study of single and double detectors on Breakout. We provide Figure 9 in Appendix F that shows the superiority of double self-supervised detectors over one single detector.

6 Discussions and Conclusion

Our detection strategies tend to degrade as the contamination ratio increases, and thus exploring detection methods in such very noisy scenarios is a promising future work. As our parametric detection framework is based on the Gaussian assumption, the investigation of other non-parametric detection strategies, such as one-class support vector machine (Choi 2009) or isolation forest (Liu, Ting, and Zhou 2008) is interesting. Lastly, we choose to directly delete the detected outliers. However, if the proportion of outliers is high, this strategy is prone to decreasing the final performance substantially. we can examine the impact of filling the deleted states via some neighboring smoothing techniques, such as *mixup* (Wang et al. 2020; Zhang et al. 2018) rather than directly deleting them in the future.

In this paper, we designed a simple yet effective outlier detection framework in the RL scenario, including Mahalanobis distance and Robust Mahalanobis distance detection strategies. Our proposed detection framework is generic, as it simultaneously considers random, adversarial and out-of-distribution states. Rigorous experiments demonstrate the efficacy of our detection strategies.

References

- Cabana, E.; Lillo, R. E.; and Laniado, H. 2021. Multivariate outlier detection based on a robust Mahalanobis distance with shrinkage estimators. *Statistical Papers*, 62(4): 1583–1609.
- Cao, Y.; Chen, X.; Yao, L.; Wang, X.; and Zhang, W. E. 2020. Adversarial attacks and detection on reinforcement learning-based interactive recommender systems. In *Proceedings of the 43rd International ACM SIGIR Conference on Research and Development in Information Retrieval*, 1669–1672.
- Chan, S. C.; Fishman, S.; Canny, J.; Korattikara, A.; and Guadarrama, S. 2019. Measuring the reliability of reinforcement learning algorithms. *International Conference on Learning Representations (ICLR)*.
- Choi, Y.-S. 2009. Least squares one-class support vector machine. *Pattern Recognition Letters*, 30(13): 1236–1240.
- Colas, C.; Sigaud, O.; and Oudeyer, P.-Y. 2018. How many random seeds? Statistical power analysis in deep reinforcement learning experiments. *arXiv preprint arXiv:1806.08295*.
- De Maesschalck, R.; Jouan-Rimbaud, D.; and Massart, D. L. 2000. The Mahalanobis distance. *Chemometrics and Intelligent Laboratory Systems*, 50(1): 1–18.
- Duan, Y.; Chen, X.; Houthooft, R.; Schulman, J.; and Abbeel, P. 2016. Benchmarking deep reinforcement learning for continuous control. In *ICML'16 Proceedings of the 33rd International Conference on International Conference on Machine Learning - Volume 48*, 1329–1338. PMLR.
- Feng, J.; Xu, H.; Mannor, S.; and Yan, S. 2013. Online PCA for contaminated data. *Advances in Neural Information Processing Systems*, 26: 764–772.
- Goodfellow, I. J.; Shlens, J.; and Szegedy, C. 2014. Explaining and harnessing adversarial examples. *International Conference on Learning Representations (ICLR)*.
- Greenberg, I.; and Mannor, S. 2021. Detecting rewards deterioration in episodic reinforcement learning. In *International Conference on Machine Learning*, 3842–3853. PMLR.
- Grübel, R. 1988. A minimal characterization of the covariance matrix. *Metrika*, 35(1): 49–52.
- Henderson, P.; Islam, R.; Bachman, P.; Pineau, J.; Precup, D.; and Meger, D. 2018. Deep reinforcement learning that matters. In *Proceedings of the AAAI Conference on Artificial Intelligence*, volume 32.
- Huang, S.; Papernot, N.; Goodfellow, I.; Duan, Y.; and Abbeel, P. 2017. Adversarial attacks on neural network policies. *Advances in Neural Information Processing Systems*.
- Huber, P. J. 2004. *Robust statistics*, volume 523. John Wiley & Sons.
- Jordan, S.; Chandak, Y.; Cohen, D.; Zhang, M.; and Thomas, P. 2020. Evaluating the performance of reinforcement learning algorithms. In *International Conference on Machine Learning*, 4962–4973. PMLR.
- Kamoi, R.; and Kobayashi, K. 2020. Why is the Mahalanobis distance effective for anomaly detection. *arXiv preprint arXiv:2003.00402*.
- Lee, K.; Lee, K.; Lee, H.; and Shin, J. 2018. A simple unified framework for detecting out-of-distribution samples and adversarial attacks. *Advances in Neural Information Processing Systems*, 31.
- Liu, F. T.; Ting, K. M.; and Zhou, Z.-H. 2008. Isolation forest. In *2008 Eighth IEEE International Conference on Data Mining*, 413–422. IEEE.
- Maronna, R. A.; and Yohai, V. J. 2014. Robust estimation of multivariate location and scatter. *Wiley StatsRef: Statistics Reference Online*, 1–12.
- Mnih, V.; Kavukcuoglu, K.; Silver, D.; Rusu, A. A.; Veness, J.; Bellemare, M. G.; Graves, A.; Riedmiller, M.; Fidjeland, A. K.; Ostrovski, G.; et al. 2015. Human-level control through deep reinforcement learning. *Nature*, 518(7540): 529–533.
- Pattanaik, A.; Tang, Z.; Liu, S.; Bommannan, G.; and Chowdhary, G. 2017. Robust deep reinforcement learning with adversarial attacks. *Advances in Neural Information Processing Systems*.
- Ren, J.; Fort, S.; Liu, J.; Roy, A. G.; Padhy, S.; and Lakshminarayanan, B. 2021. A simple fix to Mahalanobis distance for improving near-OOD detection. *arXiv preprint arXiv:2106.09022*.
- Rousseeuw, P. J. 1984. Least median of squares regression. *Journal of the American Statistical Association*, 79(388): 871–880.
- Rousseeuw, P. J.; and Van Zomeren, B. C. 1990. Unmasking multivariate outliers and leverage points. *Journal of the American Statistical Association*, 85(411): 633–639.
- Schulman, J.; Levine, S.; Abbeel, P.; Jordan, M.; and Moritz, P. 2015a. Trust region policy optimization. In *Proceedings of The 32nd International Conference on Machine Learning*, 1889–1897. PMLR.
- Schulman, J.; Moritz, P.; Levine, S.; Jordan, M.; and Abbeel, P. 2015b. High-dimensional continuous control using generalized advantage estimation. *arXiv preprint arXiv:1506.02438*.
- Schulman, J.; Wolski, F.; Dhariwal, P.; Radford, A.; and Klimov, O. 2017. Proximal policy optimization algorithms. *arXiv preprint arXiv:1707.06347*.
- Szegedy, C.; Zaremba, W.; Sutskever, I.; Bruna, J.; Erhan, D.; Goodfellow, I.; and Fergus, R. 2013. Intriguing properties of neural networks. *International Conference on Learning Representations (ICLR)*.
- Wang, K.; Kang, B.; Shao, J.; and Feng, J. 2020. Improving generalization in reinforcement learning with mixture regularization. *Advances in Neural Information Processing Systems*.
- Wilson, E. B.; and Hilferty, M. M. 1931. The distribution of chi-square. *Proceedings of the National Academy of Sciences of the United States of America*, 17(12): 684.
- Zhang, H.; Cisse, M.; Dauphin, Y. N.; and Lopez-Paz, D. 2018. mixup: Beyond empirical risk minimization. *International Conference on Learning Representations (ICLR)*.

A Proof of Proposition 1

Proof. We show that for each action class c , the Mahalanobis distance d is identically independent Chi-squared distributed under Gaussian assumption. Without loss of generality, we denote μ and Σ as the mean and variance matrix of the closest class-conditional Gaussian distribution. We need to show $d = (f(\mathbf{s}) - \mu)^\top \Sigma^{-1} (f(\mathbf{s}) - \mu)$ is Chi-squared distributed. Firstly, by eigenvalue decomposition, we have

$$\Sigma^{-1} = \sum_{k=1}^p \lambda_k^{-1} u_k u_k^\top, \quad (8)$$

where λ_k and u_k are the k -th eigenvalue and eigenvector of Σ . Plugging it into the form of d , we immediately obtain

$$\begin{aligned} d &= (f(\mathbf{s}) - \mu)^\top \Sigma^{-1} (f(\mathbf{s}) - \mu) \\ &= (f(\mathbf{s}) - \mu)^\top \left(\sum_{k=1}^p \lambda_k^{-1} u_k u_k^\top \right) (f(\mathbf{s}) - \mu) \\ &= \sum_{k=1}^p \lambda_k^{-1} (f(\mathbf{s}) - \mu)^\top u_k u_k^\top (f(\mathbf{s}) - \mu) \\ &= \sum_{k=1}^p \left[\lambda_k^{-\frac{1}{2}} u_k^\top (f(\mathbf{s}) - \mu) \right]^2 \\ &= \sum_{k=1}^p \mathbf{X}_k^2, \end{aligned} \quad (9)$$

where \mathbf{X}_k^2 is a new Gaussian variable that results from the linear transform of a Gaussian distribution $f(\mathbf{s})$ where $f(\mathbf{s}) \sim \mathcal{N}(\mu, \Sigma)$. Therefore, the resulting variance σ_k^2 can be derived as

$$\begin{aligned} \sigma_k^2 &= \lambda_k^{-\frac{1}{2}} u_k^\top \Sigma \lambda_k^{-\frac{1}{2}} u_k \\ &= \lambda_k^{-1} u_k^\top \left(\sum_{j=1}^p \lambda_j u_j u_j^\top \right) u_k \\ &= \sum_{j=1}^p \lambda_j^{-1} \lambda_j u_k^\top u_j u_j^\top u_k \end{aligned} \quad (10)$$

As the mu_j and mu_k are orthogonal if $j \neq k$, the variance σ_k^2 can be further reduced to

$$\begin{aligned} \sigma_k^2 &= \lambda_k^{-1} \lambda_k u_k^\top u_k u_k^\top u_k \\ &= \|u_k\|^2 \|u_k\|^2 \\ &= 1. \end{aligned} \quad (11)$$

Thus, each \mathbf{X}_k is a standard Gaussian distribution. Then we have the Mahalanobis distance d is Chi-squared distributed, i.e., $d \sim \chi^2(p)$, which is independent of the action class c . Without loss of generality, the smallest d over all action classes, i.e., $M(\mathbf{s})$, is also a Chi-squared distribution. That is to say, $M(\mathbf{s}) \sim \chi^2(p)$. \square

B Evaluation Phase: Main Results

We provide the main result of our detection strategies on Breakout game in Figure 10.

Also, we present main results with a 0, 0.05 and 0.1 fraction of contamination across all three games in Figure 11, 12 and 13, respectively. It reveals that robust MD-based detection method mostly outperforms classical MD detection method across different contamination ratio, even though the effectiveness of both strategies tends to reduce as the proportion of contamination increases.

C Evaluation Phase: Boxplot Results

We plot the distributions of inliers and three types of outliers on SpaceInvaders and Asterix games in Figure 14 and 15, respectively. It is worth noting that Robust MD is also capable of enlarging the separation of distributions between inliers and both random and adversarial outliers on SpaceInvaders game, while its benefits seems to be negligible on OOD outliers (Breakout) on SpaceInvaders games as well as in Asterix game. We speculate that it is determined by the game difficulty. Specifically, the PPO algorithm can achieve desirable performance on the simple Breakout game, thus yielding informative feature space vectors. By contrast, there is a room for the generalization of PPO on both SpaceInvaders and Asterix games such that Robust MD might not help while handling the less meaningful state feature vectors on these two games.

D Evaluation Phase: Sensitivity Analysis

Figure 8 manifests that there is still an ascending tendency of detection accuracy as the amount of principal components increases.

E Training Phase: Main Results

The main results for Breakout, Asterix and SpaceInvaders games in training phase are shown in Figure 16, Figure 17 and Figure 18. Results show that both of our strategies have effective detection power and thus stabilize the training of algorithms. And the hyperparameters are shown in Table 1.

F Training Phase: Ablation Study

Figure 9 reveals that compared with single detector, double self-supervised detectors can improve the detection accuracy and thus stabilize the training process. In particular, ‘‘MD Double’’ outperforms ‘‘MD Single’’ significantly, although ‘‘Robust MD Single’’ is comparable to ‘‘Robust MD Double’’.

Table 1: Hyper-parameters in training phase. RL related hyperparameters are the same as PPO.

Hyperparameter	Value
Confidence level ($1-\alpha$)	1-0.05
Moving window size (m)	2
Sample size (N_c)	5120
Iteration (K)	≈ 10000 (1e7 steps)
Environment number (N)	8
Horizon (T)	128
Feature dimension (k)	20

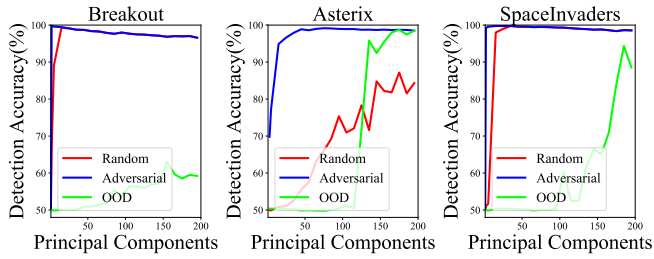


Figure 8: Detection performance under MD estimation as the number of principal components increases across Breakout, Asterix and SpaceInvaders games.

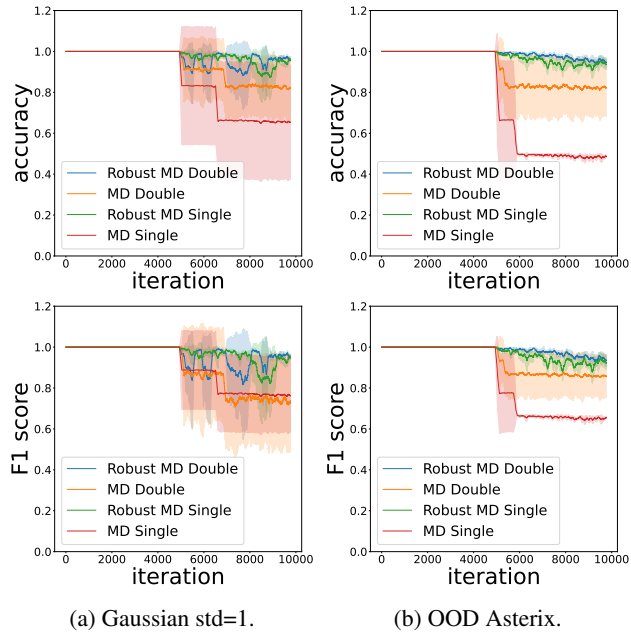


Figure 9: Accuracy and F1 score with and without double self-supervised detectors on Breakout game.

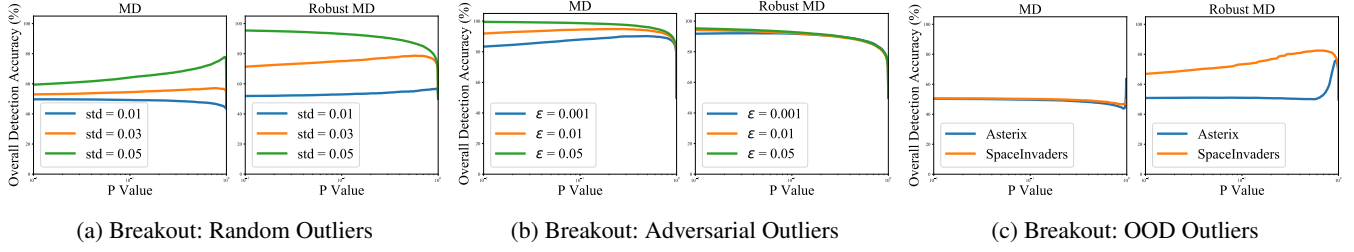


Figure 10: Detection performance on Breakout across various outliers with a 0.01 fraction of contamination.

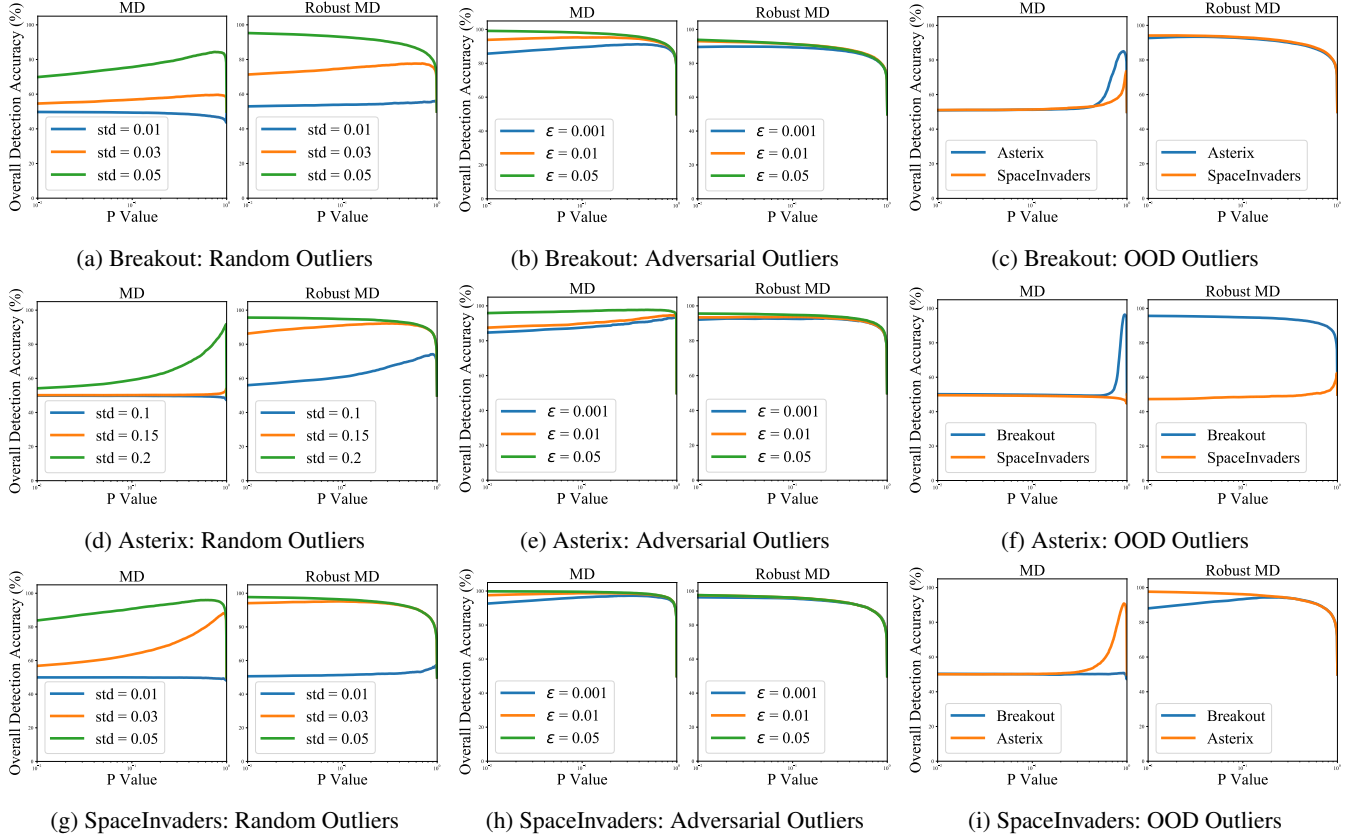


Figure 11: Detection performance in the evaluation phase across various p-value in $\chi^2_p(1-\alpha)$ on Breakout, Asterix and SpaceInvaders games with a 0 fraction of contamination (clean state while estimation).

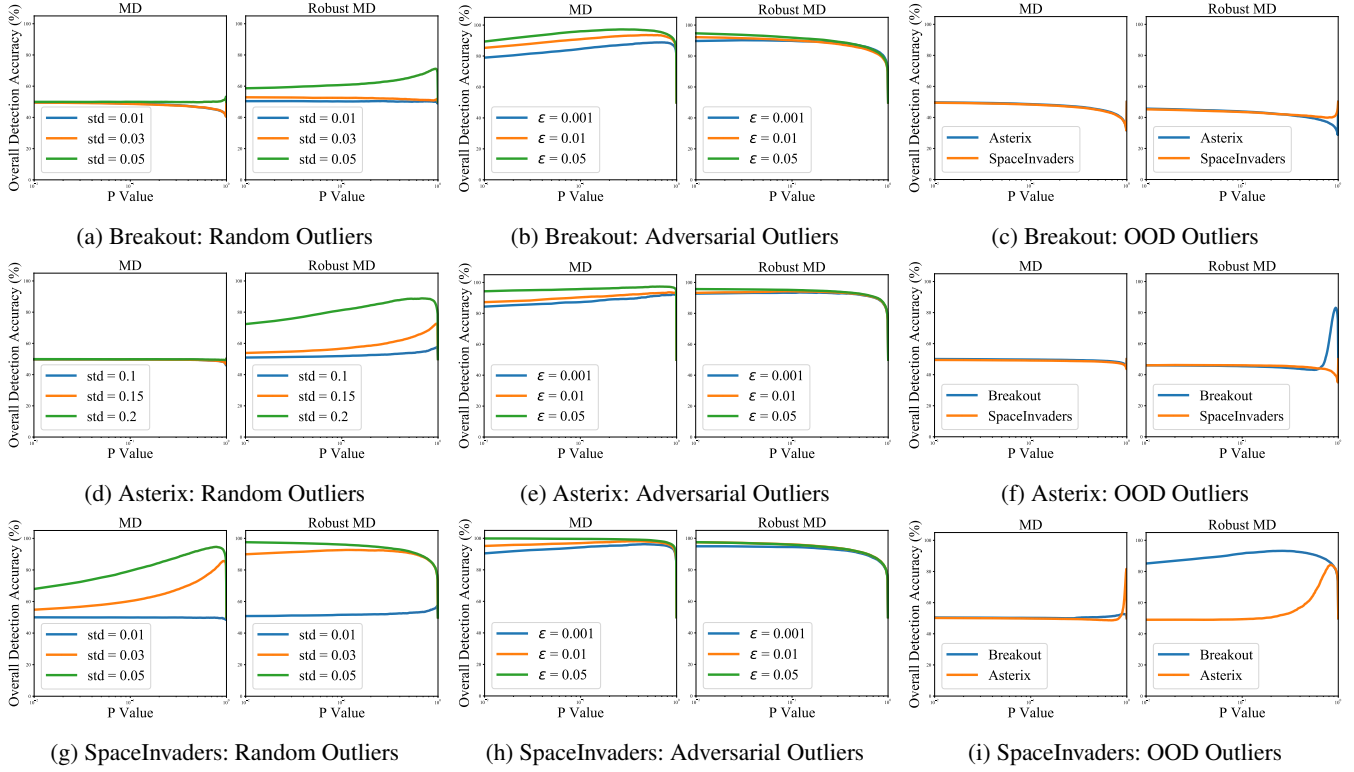


Figure 12: Detection performance in the evaluation phase across various p-value in $\chi^2_p(1-\alpha)$ on Breakout, Asterix and SpaceInvaders games with a **0.05** fraction of contamination.

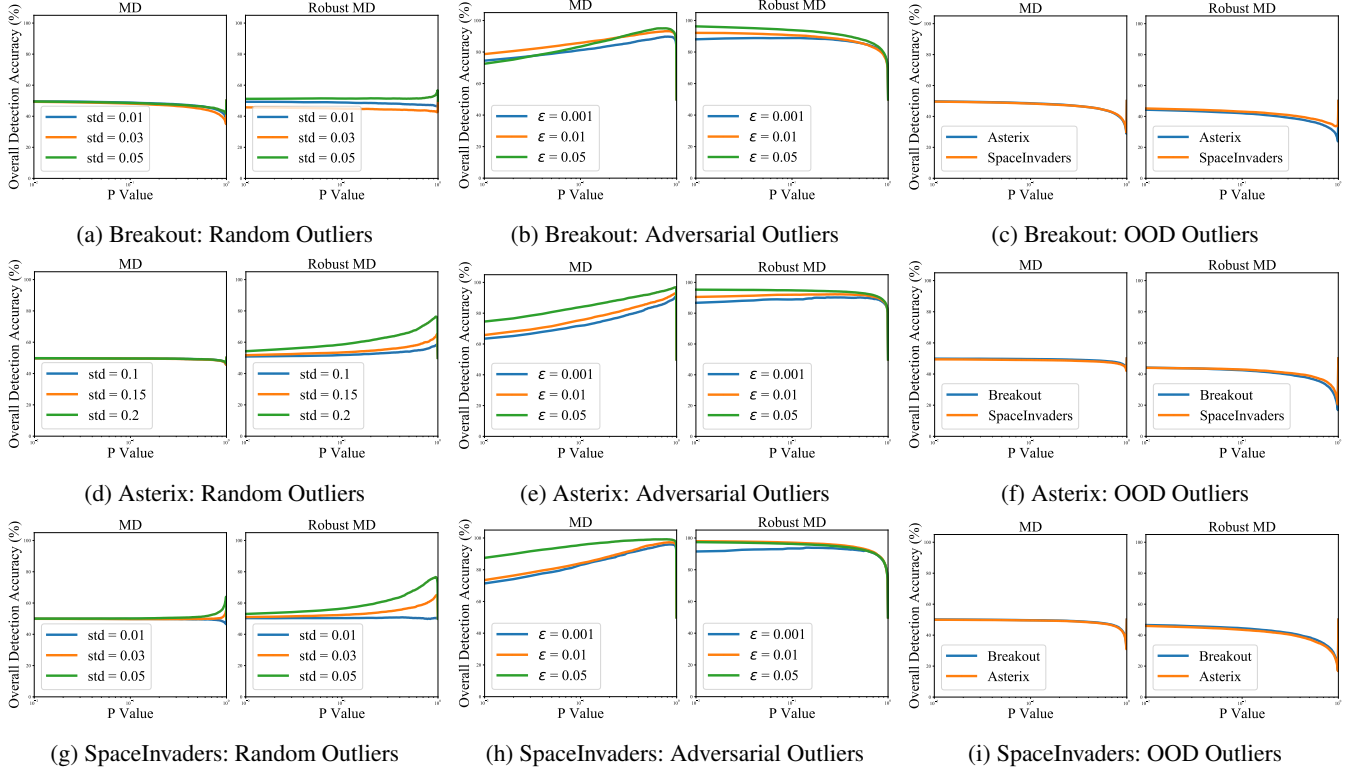


Figure 13: Detection performance in the evaluation phase across various p-value in $\chi_p^2(1-\alpha)$ on Breakout, Asterix and SpaceInvaders games with a **0.1** fraction of contamination.

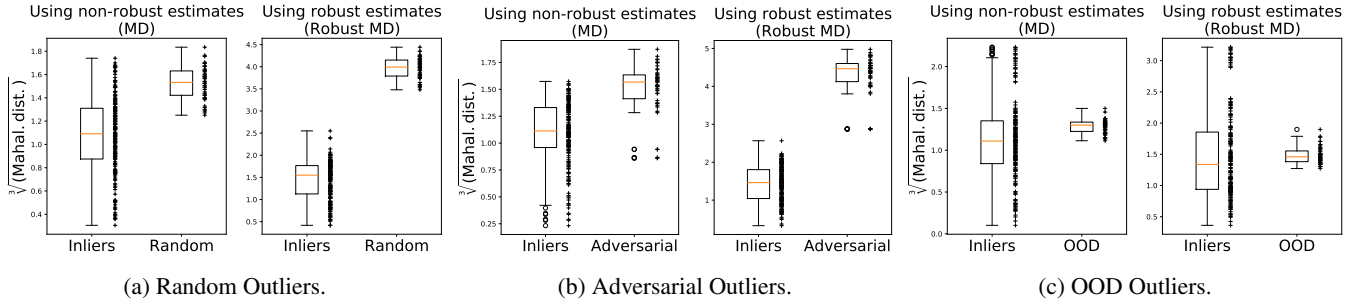


Figure 14: Boxplot of distributions between inliers and three types in a random action class on SpaceInvaders game.

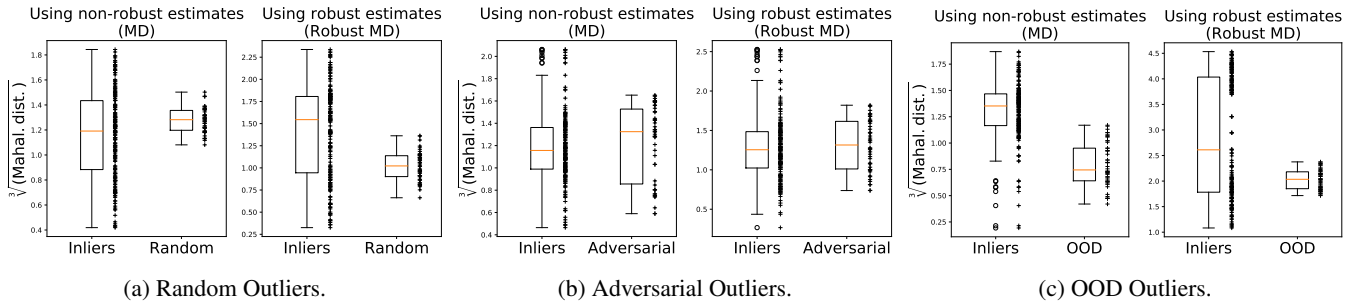


Figure 15: Boxplot of distributions between inliers and three types in a random action class on Asterix game.

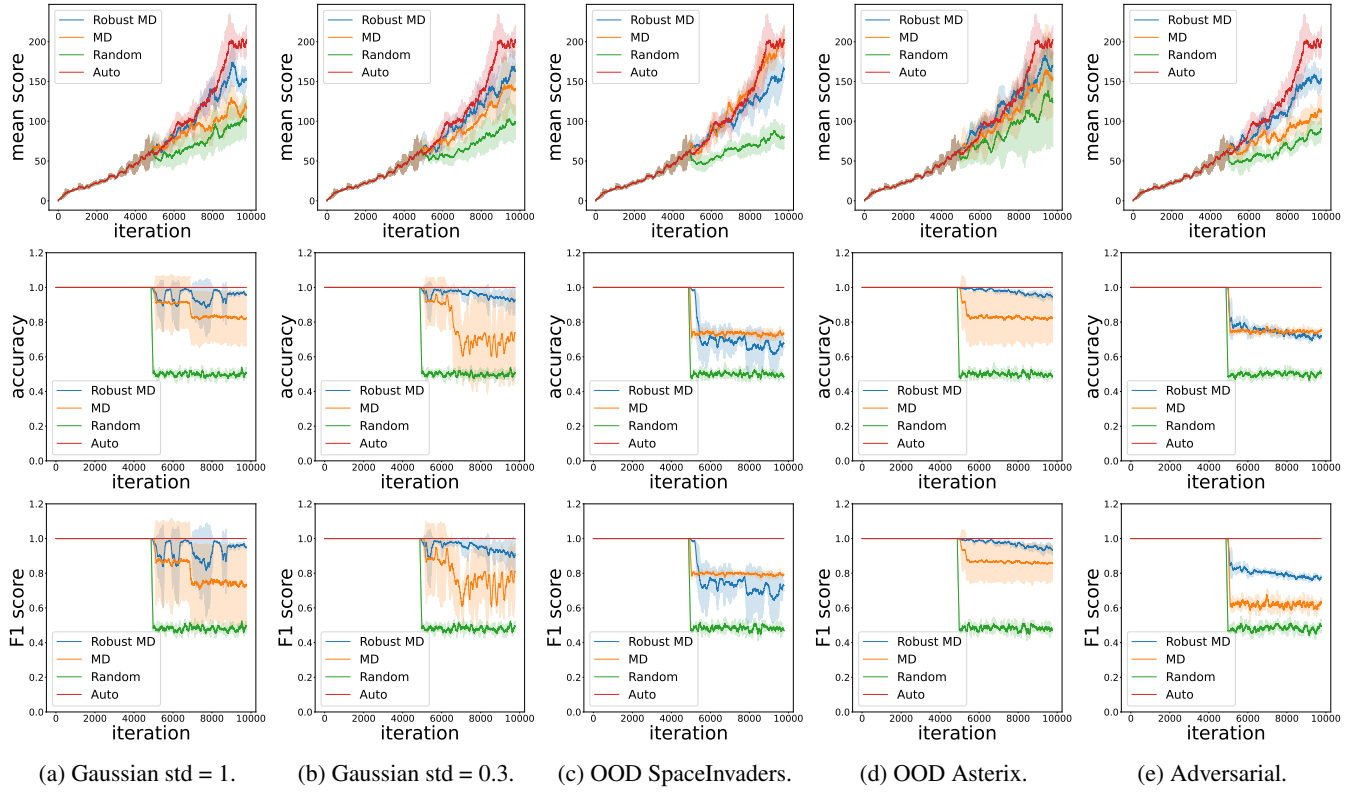


Figure 16: Anomaly detection in training phase on Breakout game.

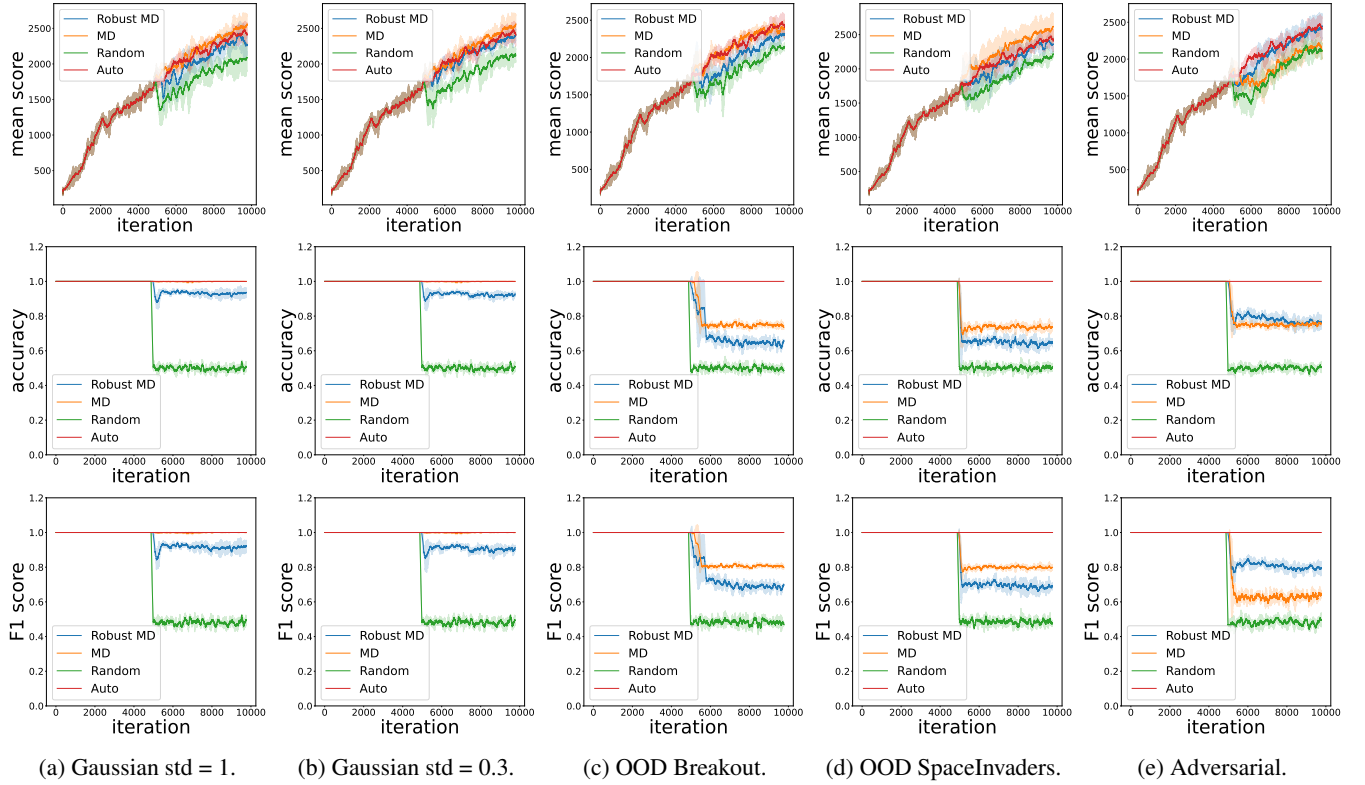


Figure 17: Anomaly detection in training phase on Asterix game.

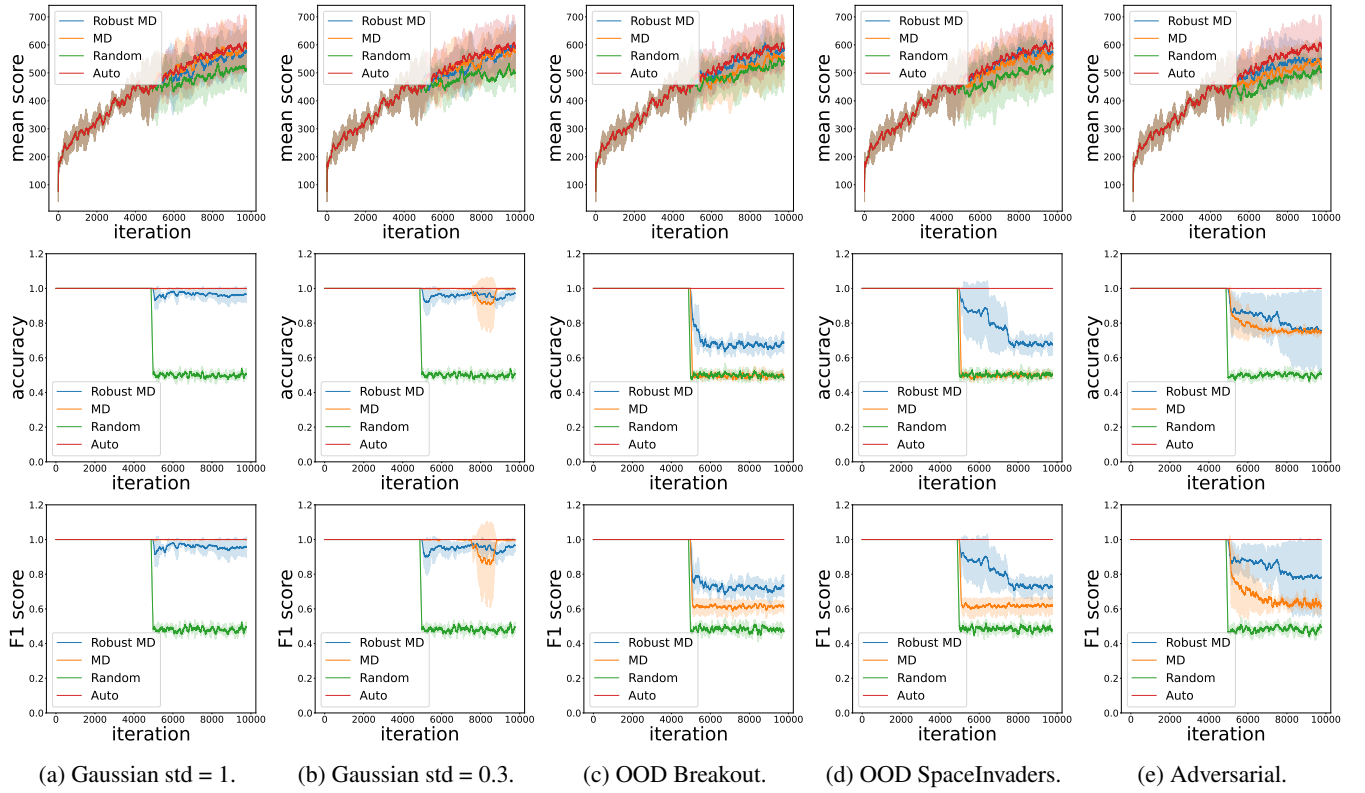


Figure 18: Anomaly detection in training phase on SpaceInvaders game.